Available online at www.sciencedirect.com
SCIENCE DIRECT®

Polymer 44 (2003) 7573–7588

polymer

www.elsevier.com/locate/polymer

Synthesis and properties of thermoplastic elastomers based on PTMO and tetra-amide

J. Krijgsman, D. Husken, R.J. Gaymans*,[1]

Department of Chemical Technology, Laboratory of Polymer Technology, University of Twente, P.O. Box 217, 7500 AE Enschede, Netherlands

Received 13 November 2002; received in revised form 15 September 2003; accepted 24 September 2003

Abstract

Segmented copolymers based on T6T6T-dimethyl (two-and-a-half repeating unit of nylon-6,T) and PTMO or extended PTMO_{1000}/DMT that are thermoplastic elastomers were made via polycondensation. The materials have a good solvent resistance, are melt-processable and transparent. The polymers all have a low glass transition temperature (− 60 to − 0 °C). The rubbery plateau is wide and extremely flat and the melting temperature is sharp and high. The shear modulus of the rubbery plateau (3.3–14.5 MPa) and the flow temperature (183–220 °C) increase with increasing T6T6T content (5–16 wt%), corresponding to increasing crystallinity. The undercooling, as measured by DSC, is 20–30 °C. The compression set at room temperature is low (6–7%) and decreases slightly with decreasing T6T6T content. With AFM it was shown that the crystalline T6T6T units form long threads or ribbon like structures with a high aspect ratio in the amorphous PTMO matrix.
© 2003 Elsevier Ltd. All rights reserved.

Keywords: Thermoplastic elastomer; PTMO; Tetra-amide

1. Introduction

Thermoplastic elastomers (TPE's) [1,2] are polymers that show elastomeric behaviour at their service temperature and that can be melt-processed at elevated temperatures. A special kind of thermoplastic elastomers are segmented copolymers or multi-block copolymers that consist of alternating hard segments and amorphous soft segments that phase separate. The hard segment domains act as physical crosslinks for the copolymer.

Segmented copolymers that are crystallised from a homogeneous melt can form spherulitic structures [3]. However, at fast cooling rates (high nucleation rates) and low concentration (<20 wt%) intermeshing bundles of lamellae (ribbons) with a high aspect ratio are formed [3–6]. The crystallisation of the hard segment can be improved by using uniform crystallisable hard segments [7–10]. Uniform hard segments crystallise faster and more complete into crystallites with sharp boundaries and a constant melting temperature.

Previous research on segmented copolymers having uniform crystallisable amide units focused on T6T–PTMO [11], T4T–PTMO [12], T2T–PTMO [13] and TΦT–PTMO [6,14–16] (Fig. 1). Poly(tetramethylene oxide) (PTMO) is used as amorphous segment. The T6T, T4T, T2T and TΦT uniform crystallisable units are di-amide segments based on 1,6-hexanediamine (6), 1,4-butanediamine (4), 1,2-ethanediamine (2) or *p*-phenylenediamine (Φ) and dimethyl terephthalate (T).

The crystallisable segments are extremely short (~2 nm) and crystallise fast and almost complete, resulting in a two-phase structure with good properties. The melting temperature increases with increasing hard segment rigidity and lamellar thickness [17]. The fast crystallisation is possibly due to the fact that the di-amide units remain organised in the melt [12,18–22] and probably form nano-ordered phases. With increasing amide segment content the melting temperature, modulus at room temperature and yield stress increase [6,11–16]. With increasing molecular weight the tensile stress and strain increase due to an increased number of entanglements per chain [6].

The length and type (regularity) of amorphous segment is important as it influences the strain-induced crystallisation. Regular PTMO segments longer than 2000 g/mol show strong strain hardening above 300% strain. It was found that the length of the amorphous segment in PTMO_{1000} extended

---

* Corresponding author.
E-mail address: r.j.gaymans@utwente.nl (R.J. Gaymans).

[1] Present address: KEMA Nederland B.V., Arnhem, The Netherlands.

0032-3861/$ - see front matter © 2003 Elsevier Ltd. All rights reserved.
doi:10.1016/j.polymer.2003.09.043

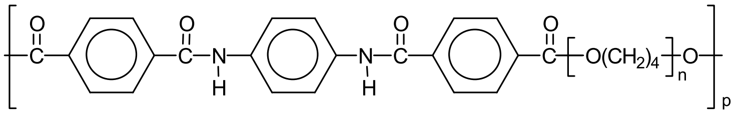

Fig. 1. Structure of TΦT–PTMO segmented copolymer.

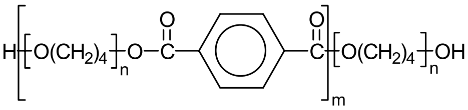

Fig. 2. Structure of PTMO extended with DMT. The value of *n* determines the PTMO length, *m* determines the length of extended PTMO/DMT.

with dimethyl terephthalate (PTMO/DMT, Fig. 2) seems to have little effect on the extent of strain hardening [15].

The properties of TΦT–($PTMO_{1000}$/DMT) segmented copolymers, as function of the $PTMO_{1000}$/DMT length and structure, have been studied thoroughly [6,14–16]. However, very soft materials with a good elasticity and high melting temperature do not exist, as di-amide units with a higher melting temperature than the fully aromatic TΦT are not known. The melting temperature can be increased by using di-amide segments that are extended via a diol [11, 23–25], because the lamellar thickness of such extended segments is higher [17]. Copolymers with diol-extended di-amides have a higher melting temperature, but the melting temperature is broadened and also melt phasing occurs. This is caused by the length distribution in the diol-extended di-amides.

In this article the synthesis and structure-property relationships of segmented copolymers based on PTMO as amorphous segment and T6T6T-dimethyl as crystallisable segment will be discussed. T6T6T-dimethyl is a new crystallisable unit (tetra-amide) based on two-and-a-half repeating units of nylon-6,T [26]. The structure of the bisester tetra-amide T6T6T-dimethyl, having methyl ester endgroups, is given in Fig. 3.

The T6T6T tetra-amide segment can form four hydrogen bonds as compared to the T6T segment and other di-amide segments that can only form two hydrogen bonds. The lamellar thickness will be higher and the melting temperature is expected to be higher than with di-amide units [17]. The expectation is that copolymers of PTMO with tetra-amide units show better elasticity than copolymers with di-amide units because it is more difficult to shear the thicker T6T6T crystallites.

2. Experimental

2.1. Materials

Dimethyl terephthalate (DMT) and *N*-methyl-2-pyrrolidone (NMP) were purchased from Merck and used as received. Tetra-isopropyl orthotitanate ($Ti(i\text{-}OC_3H_7)_4$), purchased from Merck, was diluted in anhydrous *m*-xylene (to 0.05 M), obtained from Fluka. Poly(tetramethylene oxide) (PTMO, 1000, 2000 and 2900 g/mol) was provided by DuPont. Irganox 1330 was obtained from CIBA. T6T6T-dimethyl was synthesised from DMT, MPT (methyl phenyl terephthalate) and 1,6-hexamethylenediamine (HMDA) [26].

2.2. Synthesis of T6T6T–PTMO

The T6T6T–PTMO copolymers were synthesised by a polycondensation reaction [14] using PTMO of different lengths and T6T6T-dimethyl. The preparation of T6T6T–$PTMO_{2000}$ is given as an example.

The reaction was carried out in a 250 ml stainless steel reactor with a nitrogen inlet and mechanical stirrer. The vessel was loaded with T6T6T-dimethyl (6.86 g, 10 mmol), $PTMO_{2000}$ (20.0 g, 20 mmol), Irganox 1330 (0.2 g), 100 ml NMP and catalyst solution (2 ml of 0.05 M $Ti(i\text{-}OC_3H_7)_4$ in *m*-xylene). This mixture was first heated in an oil bath to 180 °C under nitrogen flow. After 30 min reaction time, the temperature was raised to 220 °C and after another 30 min to 250 °C and maintained for 2 h. The pressure was then carefully reduced ($P < 20$ mbar) to distil off the NMP during 30 min and then further reduced ($P < 1$ mbar) for 60 min. During this last hour, the temperature was first raised to 280 °C for 15 min and reduced to 250 °C for the final 45 min. Finally, the vessel was allowed to slowly cool to room temperature whilst maintaining the low pressure. Then the polymer was cooled with liquid nitrogen, cut out of the reactor and crushed.

2.3. Synthesis of T6T6T–($PTMO_{1000}$/DMT)

The T6T6T–($PTMO_{1000}$/DMT) copolymers were

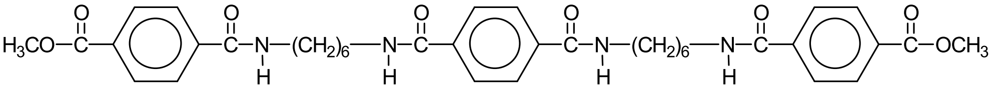

Fig. 3. Structure of the crystallisable segment T6T6T-dimethyl.

synthesised by a polycondensation reaction [14] using PTMO (1000 g/mol) extended with DMT and T6T6T-dimethyl. The preparation of T6T6T–(PTMO$_{1000}$/DMT)$_{3000}$ (PTMO of 1000 g/mol extended to 3000 g/mol with DMT) is given as an example.

The reaction was carried out in a 250 ml stainless steel reactor with a nitrogen inlet and mechanical stirrer. The vessel was loaded with T6T6T-dimethyl (6.86 g, 10.0 mmol), PTMO$_{1000}$ (27.7 g, 27.7 mmol), DMT (3.44 g, 17.7 mmol), Irganox 1330 (0.3 g), 100 ml NMP and catalyst solution (3 ml of 0.05 M Ti(i-OC$_3$H$_7$)$_4$ in m-xylene). This mixture was first heated in an oil bath to 180 °C under nitrogen flow. After 30 min reaction time, the temperature was raised to 220 °C and after another 30 min to 250 °C and maintained for 2 h. The pressure was then carefully reduced ($P < 20$ mbar) to distil off the NMP and then further reduced ($P < 1$ mbar) for 60 min. Finally, the vessel was allowed to slowly cool to room temperature whilst maintaining the low pressure. Then the polymer was cooled with liquid nitrogen, cut out of the reactor and crushed.

2.4. Viscometry

The inherent viscosity of the polymers was determined with a capillary Ubbelohde type 1B at 25 °C, using a polymer solution with a concentration of 0.1 g/dl in phenol/1,1,2,2-tetrachloroethane (50/50, mol/mol). The inherent viscosity is used as a measure for the molecular weight of the polymers.

2.5. DMA

Samples for the DMA test ($70 \times 9 \times 2$ mm^3) were prepared on an Arburg-H manual injection moulding machine. Before use, the samples were dried in a vacuum oven at 70 °C overnight. The torsion behaviour (G' and G'' versus temperature) was studied at a frequency of 1 Hz, a strain of 0.1% and a heating rate of 1 °C/min using a Myrenne ATM3 torsion pendulum. The glass transition temperature (T_g) was expressed as the temperature where the loss modulus G'' has a maximum. The flow temperature (T_{flow}) was defined as the temperature where the storage modulus G$'$ reached 1 MPa. The storage modulus of the rubbery plateau is determined at room temperature (G'(25 °C)).

2.6. Compression set

A piece of an injection moulded test bar (~2.15 mm thickness), was placed between two steel plates and compressed to 1 mm (~55% compression) or 1.6 mm (~25% compression). After 24 h at 20 or 70 °C the compression was released. One hour later the thickness of the sample was measured. The compression set (CS) was defined as:

$$\text{Compression set} = \frac{d_0 - d_2}{d_0 - d_1} \times 100\% \quad [\%] \qquad (1)$$

with:

d_0, thickness before compression (mm)
d_1, thickness during compression (mm)
d_2, thickness 1 h after release of compression (mm).

2.7. DSC

DSC spectra were recorded on a Perkin–Elmer DSC7 apparatus, equipped with a PE7700 computer and TAS-7 software. Dried samples of 5–10 mg polymer were measured with a heating and cooling rate of 20 °C/min. The samples were heated to 300 °C, kept at that temperature for 2 min, cooled to 50 °C and reheated to 300 °C. The (peak) melting temperature and enthalpy were taken from the second heating scan. The crystallisation temperature was taken as the maximum of the peak in the cooling scan.

2.8. WAXD

X-ray diffraction data of melt-pressed samples were collected with a Philips PW3710 based X'Pert-1 diffractometer in Bragg-Brentano geometry, using a Θ compensating divergence slit (12.5 mm length). Diffraction data collection was performed at room temperature, using a low-background spinning (1 r/s) specimen holder. Cu K$_{\alpha 1}$ radiation of 1.54056 Å was obtained with a curved graphite monochromator. The data were collected in a range of $2\Theta = 4 - 60°$.

Melt-pressed samples of $10 \times 15 \times 1$ mm^3 were prepared from an injection-moulded test bar in a mould at 280 °C for 5 min with a pressure of 10 bar, after which the samples were slowly cooled with 5 °C/min.

2.9. AFM

AFM measurements were performed on a Nanoscope III A (Veeco/Digital Instruments) AFM in tapping mode. The AFM was equipped with a D-scanner with a maximum scan size of 15 μm^2. Commercially available Si-cantilevers (Nanosensors) were used to obtain the height and phase images.

Solution cast samples of ~1 μm thickness on glass were prepared from a 1 wt% solution in NMP (100 °C) and dried at 100 °C during one night. Bulk samples (solidified from the melt) were taken from the wall of the reaction vessel after cooling slowly to room temperature and used as such.

3. Results and discussion

3.1. Synthesis

Copolymers based on T6T6T-dimethyl and PTMO or

PTMO extended with DMT were synthesised via a polycondensation reaction. The first part of the polymerisation reaction was carried out in NMP solution, because of the high melting temperature of T6T6T-dimethyl (303 °C) [26]. The melting temperature of T6T6T decreases after reaction with PTMO. Therefore, after 2 h at 250 °C the reaction had progressed enough to allow the final part of the reaction to be performed in the melt. A vacuum of <1 mbar was applied during the last hour to strip off any methanol formed and to obtain polymers with high molecular weights. For high T6T6T content (PTMO length <3000 g/mol) the temperature was raised to 280 °C for 15 min during the last stage of the reaction to get a homogeneous, clear melt. The yield was $>98\%$.

Three series of segmented copolymers based on T6T6T-dimethyl and PTMO were made:

1. Uniform T6T6T-dimethyl with PTMO of different lengths (2000 and 2900 g/mol).
2. Uniform T6T6T-dimethyl with extended PTMO of 1000 g/mol with a PTMO_{1000}/DMT length of 3000–10,000 g/mol.
3. T6T6T-dimethyl with a uniformity of $\sim 76\%$ (76 mol% T6T6T-dimethyl and 24 mol% T(6T)_n with $n > 2$) with PTMO_{1000}/DMT of 3000–6000 g/mol. The uniformity of the tetra-amide segment is defined as the percentage of T6T6T-dimethyl in the starting material. When the uniformity is below 100%, part of the product consists of side products such as T6T6T6T-dimethyl or T6T6T6T6T-dimethyl [26].

The copolymers could be easily obtained with high molecular weights (inherent viscosity >1 dl/g), but it was more difficult to obtain high molecular weight (>2 dl/g) with non-uniform T6T6T. Irganox 1330 is well suitable in this reaction as there are no signs of degradation of PTMO, despite the high reaction temperature. With NMR it was shown that the uniformity of the tetra-amide segments is preserved in the copolymer. The solvent resistance of the materials is very good, as they are only soluble at low concentration and after long time in solvents such as a 50/50 mixture of phenol/1,1,2,2-tetrachloroethane, trifluoro acetic acid or NMP (above 100 °C). Furthermore, the materials are transparent, which indicates that the crystallite sizes are very small (no spherulites) and that no liquid–liquid demixing or melt phasing has occurred [14]. The materials have a faint yellow colour. The intensity of the colour decreases with increasing soft segment length.

3.2. Thermal–mechanical properties

The polymers were injection moulded into bars and dried in a vacuum oven at 70 °C. The thermal–mechanical properties were measured by DMA. The results are given in Table 1. The T6T6T content was calculated, assuming that the ester carbonyl does not crystallise and belongs to the amorphous phase [18]. The results of the three different series will be discussed successively.

3.2.1. Series 1: T6T6T–PTMO

T6T6T–PTMO copolymers based on uniform T6T6T and PTMO of 2000 and 2900 g/mol were made. The thermal–mechanical properties as studied by DMA are given in Table 1 and Fig. 4.

The hard segment content decreases with increasing soft segment length, due to the uniform length of the hard segments. Both copolymers show a rather broad glass and melting transition of the PTMO phase, a sharp flow temperature of the T6T6T phase and a wide and temperature-independent rubbery plateau. The modulus of the rubbery plateau, the loss modulus and the flow temperature increase with increasing T6T6T content, due to increased crystallinity.

The glass transition temperature is determined as the maximum of the loss modulus G''. The T_g of the copolymers with PTMO of 2000 and 2900 g/mol is -70 °C, which is close to the T_g of pure PTMO (-86 °C) [27]. The low and constant glass transition temperature of PTMO in the copolymer suggests that little amorphous T6T6T is being mixed with PTMO [14] and thus that crystallisation of T6T6T is almost complete. The shoulder in the modulus after the glass transition at -50 to 0 °C is a result of the presence of a PTMO crystalline phase that melts at this temperature. Especially longer PTMO segments above 1400 g/mol are able to crystallise [14,15].

The DMA data do not show the presence of a second T_g which can be ascribed to the presence of a separate amorphous T6T6T phase (T_g nylon-6,T $= 125$ °C [28]). Thus all T6T6T that is pre-ordered in the melt crystallises and the part of the T6T6T units that does not crystallise mixes with the amorphous PTMO phase.

The flow temperature is defined as the temperature where the storage modulus G' reaches 1 MPa. The flow temperature is 0–10 °C lower than the melting temperature. The flow temperature is more close to the melting temperature when the flow temperature is sharp. The copolymers of series 1 show a sharp flow temperature. This can be explained by the formation of perfect, uniform lamellae from uniform T6T6T. Lamellae of uniform thickness melt in a narrow temperature range. The T_{flow} decreases with decreasing T6T6T content. This result is in agreement with what has been observed in other systems [11–15]. This effect has been explained by the solvent effect theory of Flory [29]. The degree of crystallinity increases when the T6T6T content increases or when the PTMO length decreases. The flow temperature of the T6T6T segmented copolymers is considerably higher than the T_{flow} of the T6T–PTMO [11] copolymers and other di-amide copolymers [12–15]. Copolymers based on tetra-amide

Table 1

Thermal–mechanical properties as measured by DMA for: T6T6T–PTMO copolymers with uniform T6T6T (series 1), T6T6T–($PTMO_{1000}$/DMT) with uniform T6T6T (series 2) and T6T6T–($PTMO_{1000}$/DMT) with T6T6T with a uniformity of 76% (series 3)

	T6T6T content (wt%)	η_{inh} (dl/g)	T_g (°C)	G'(25°C) (MPa)	T_{flow} (°C)
Series 1: uniform					
T6T6T–$PTMO_{2000}$	22	2.2	−70	34	226
T6T6T–$PTMO_{2900}$	16	2.7	−70	17	216
Series 2: uniform					
T6T6T–$(PTMO_{1000}/DMT)_{3000}$	15.7	3.1	−61	14.5	220
T6T6T–$(PTMO_{1000}/DMT)_{4000}$	12.3	2.3	−60	8.5	208
T6T6T–$(PTMO_{1000}/DMT)_{6000}$	8.6	2.6	−61	6.8	200
T6T6T–$(PTMO_{1000}/DMT)_{8000}$	6.6	2.2	−63	5.1	190
T6T6T–$(PTMO_{1000}/DMT)_{10,000}$	5.4	2.5	−63	3.3	183
Series 3: non-uniform					
T6T6T–$(PTMO_{1000}/DMT)_{3000}$	15.7	1.4	−60	23.5	242
T6T6T–$(PTMO_{1000}/DMT)_{4000}$	12.3	1.5	−61	14.3	240
T6T6T–$(PTMO_{1000}/DMT)_{6000}$	8.6	1.9	−61	6.9	210

crystallisable segments have higher melting temperatures in the copolymer compared to di-amide segments.

The modulus of the rubbery plateau is constant over a wide temperature range. This is also a result of the formation of perfect crystalline lamellae with T6T6T. When some of the crystallites would melt at a lower temperature, a decrease in modulus with temperature would be expected.

3.2.2. Series 2: T6T6T–($PTMO_{1000}$/DMT) (uniform T6T6T)

A polymer series of T6T6T–($PTMO_{1000}$/DMT) with uniform T6T6T and $PTMO_{1000}$/DMT of 3000–10,000 g/mol was made. The thermal–mechanical properties as studied by DMA are given in Table 1 and Fig. 5.

All polymers of series 2 show a sharp glass transition of the $PTMO_{1000}$/DMT phase, a sharp flow temperature of the T6T6T phase and a wide and temperature-independent rubbery plateau. The glass transition temperature of $PTMO_{1000}$/DMT is independent of the T6T6T content, which suggests that little T6T6T is dissolved in this phase and that this amount is independent of the T6T6T content.

With increasing T6T6T content the rubber modulus and flow temperature increase due to increased crystallinity as was explained for series 1. The influence of T6T6T content on T_g, rubber modulus and T_{flow} will be discussed in more detail later.

The loss modulus is very low for all copolymers of series 2, except for T6T6T–$(PTMO/_{1000}DMT)_{3000}$ that shows a somewhat higher G''. This indicates that the elasticity decreases with increasing T6T6T content.

In Fig. 6 the storage and loss modulus of T6T6T–$(PTMO/_{1000}DMT)_{3000}$ are compared with those of T6T6T–$PTMO_{2900}$. Both have about the same T6T6T content. The T_g is in general a little higher (5–10 °C) for extended $PTMO_{1000}$ than for copolymers of series 1 with regular PTMO. This is caused by the incorporation of the terephthalic unit in the PTMO amorphous phase, which

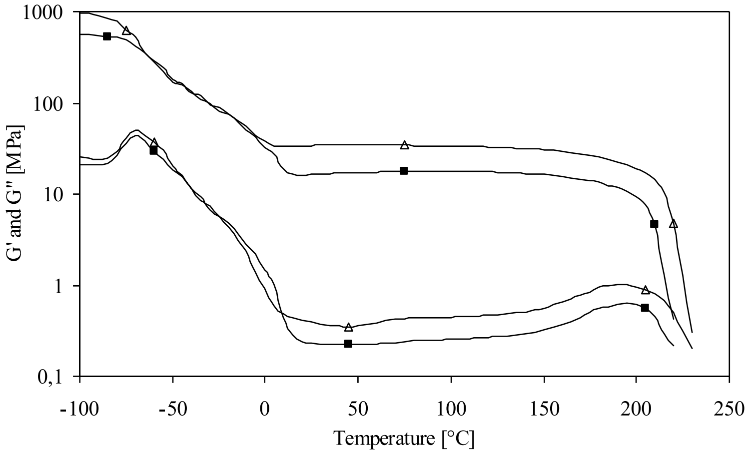

Fig. 4. Storage and loss modulus of T6T6T–PTMO copolymers with different soft segment lengths and uniform T6T6T (series 1): (△), 2000 g/mol; (■), 2900 g/mol.

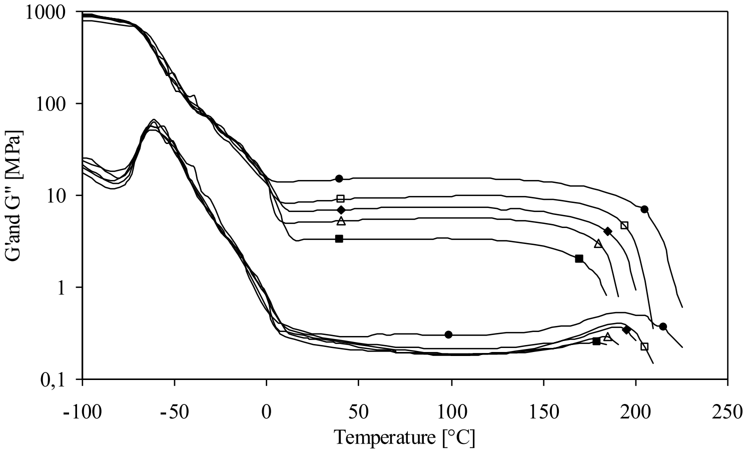

Fig. 5. Storage and loss modulus of T6T6T–($PTMO_{1000}$/DMT) copolymers with different soft segment lengths and uniform T6T6T (series 2): (●), 3000 g/mol; (□), 4000 g/mol; (◆), 6000 g/mol; (△), 8000 g/mol; (■), 10,000 g/mol.

makes this phase a little less flexible. When the segmental mobility decreases, the T_g increases. The same difference between regular and extended PTMO was found for copolymers with aromatic di-amides as crystallisable unit [14,15].

Both copolymers based on regular $PTMO_{2900}$ or extended $PTMO_{1000}$/DMT of 3000 g/mol show a shoulder in the modulus after the glass transition at −50 to 0 °C as a result of the presence of a PTMO crystalline phase. The shoulder is smaller for extended PTMO than regular PTMO of the same length. $PTMO_{1000}$/DMT is less easy to crystallise [15].

The modulus in the rubbery plateau and the flow temperature of T6T6T–$PTMO_{2900}$ and T6T6T–$(PTMO_{1000}/DMT)_{3000}$ are comparable, which indicates that the degree of crystallinity and crystalline morphology of both copolymers are equal.

In Fig. 7 the modulus is given as function of temperature for T6T6T–$(PTMO_{1000}/DMT)_{3000}$, compared to two other copolymers based on extended $PTMO_{1000}$/DMT and the di-amide segment TΦT (Fig. 1) as crystallisable segment [15]. TΦT is based on one-and-a-half repeating unit of poly-(*p*-phenylene terephthalamide). In TΦT–$(PTMO_{1000}/DMT)_{1500}$ the content of crystallisable units (16 wt%) is the same as in T6T6T–$(PTMO_{1000}/DMT)_{3000}$. In TΦT–$(PTMO_{1000}/DMT)_{3000}$ (9 wt% TΦT) the soft segment length between two crystallisable units (3000 g/mol) is the same as in T6T6T–$(PTMO_{1000}/DMT)_{3000}$ (16 wt% T6T6T) and as a result the hard segment content with TΦT is lower. The T6T6T and TΦT polymers with an amorphous segment length of 3000 g/mol have the same molar content of amide units and thus at constant molecular weight the same number of physical crosslinks per chain (network density).

Fig. 7 shows that the glass transition temperature is 5 °C lower with TΦT as compared to T6T6T in $PTMO_{1000}$/DMT. This indicates that more T6T6T than TΦT can dissolve in the amorphous PTMO phase. Probably T6T6T has more interaction with the $PTMO_{1000}$/DMT phase than TΦT. As a result the phase separation is a little less complete and part of the T6T6T is present in the amorphous phase.

As a result of the increased T_g with T6T6T the rubbery plateau for T6T6T–$(PTMO_{1000}/DMT)_{3000}$ starts at a higher

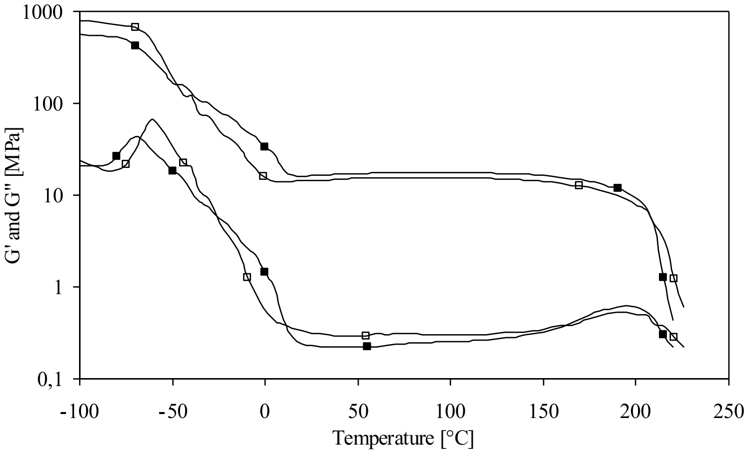

Fig. 6. Storage and loss modulus of copolymers of series 1 and 2 with soft segment length around 3000 g/mol and uniform T6T6T: (■), T6T6T–$PTMO_{2900}$ (series 1); (□), T6T6T–$(PTMO_{1000}/DMT)_{3000}$ (series 2).

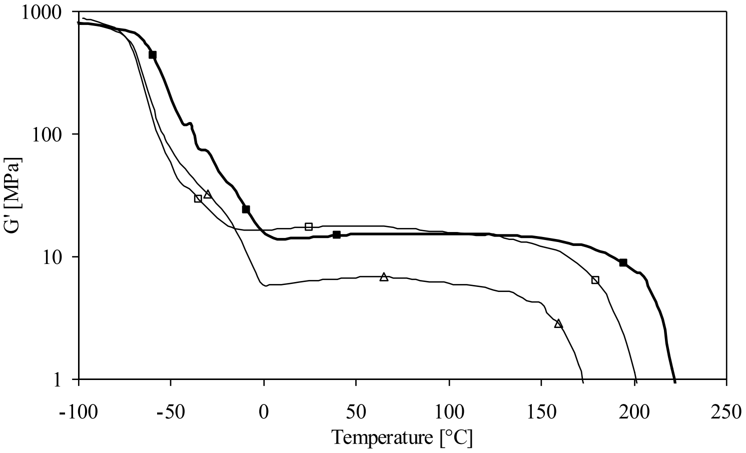

Fig. 7. Storage modulus of copolymers with $PTMO_{1000}$/DMT soft segment and T6T6T compared to TΦT as crystallisable segment: (■), T6T6T–$(PTMO_{1000}/DMT)_{3000}$; (△), TΦT–$(PTMO_{1000}/DMT)_{3000}$ (same molar content amide) [15]; (□) TΦT–$(PTMO_{1000}/DMT)_{1500}$ (same weight content amide) [15].

temperature than with TΦT. For some applications it is important that the material has constant properties down to very low temperatures.

The modulus of the rubbery plateau is influenced by the crystallinity (reinforcement by fibres or crystalline ribbons) and the network density. A polymer with 16 wt% T6T6T ($PTMO_{1000}$/DMT of 3000 g/mol) has the same modulus as a polymer with 16 wt% TΦT ($PTMO_{1000}$/DMT of 1500 g/mol). The modulus of the TΦT–$(PTMO_{1000}/DMT)_{3000}$ (9 wt% TΦT) copolymer is much lower than that of T6T6T–$(PTMO_{1000}/DMT)_{3000}$ (16 wt% T6T6T). The modulus of the rubbery plateau is thus determined predominately by the weight content of amide units. The crystallinity of the amide units in both copolymers with 16 wt% amide units is expected to be about the same, since the rubber moduli are the same. It was however, expected that the crystallinity of T6T6T–$(PTMO_{1000}/DMT)_{3000}$ would be a little lower, because the T_g of this polymer was higher as a result of more mixing with amorphous T6T6T. Therefore, probably only a small percentage of the 16 wt% of T6T6T is dissolved in the amorphous $PTMO_{1000}$/DMT phase.

With 16 wt% T6T6T the flow temperature is about 20 °C higher than with 16 wt% TΦT. The melting temperature of TΦT-dimethyl is 371 °C [14] and that of T6T6T-dimethyl is 303 °C [26]. Apparently the solvent effect of PTMO is lower for T6T6T than for TΦT. This is due to the higher lamellar thickness of crystalline ribbons of T6T6T. The more the segment length approaches that of the homopolymer of the crystalline segment, the smaller the solvent effect of the amorphous phase [29].

3.2.3. Series 3: T6T6T–($PTMO_{1000}$/DMT) (uniformity 76%)

In Fig. 8 and Table 1 an overview of the thermal–mechanical properties as measured by DMA of the T6T6T–($PTMO_{1000}$/DMT) copolymers with T6T6T-dimethyl of low uniformity (76%) is given. This T6T6T-dimethyl consists for 76 mol% of T6T6T-dimethyl and 24 mol% of $T(6T)_n$ with $n > 2$. It is more difficult to obtain high molecular weight polymers when non-uniform T6T6T is used because it is not possible to calculate the amount of reactants in stoichiometry.

The effect of T6T6T content on T_g, rubbery plateau and T_{flow} in polymers based on non-uniform T6T6T and $PTMO_{1000}$/DMT is comparable with that using uniform T6T6T (series 2). The T_g is constant and the rubbery plateau and flow temperature increase with increasing T6T6T content. Also the loss modulus increases with increasing T6T6T content, especially for the higher T6T6T content. The only difference with series 2 is that the flow temperature with non-uniform T6T6T is shows a traject. The influence of T6T6T content on T_g, rubber modulus and T_{flow} will be discussed in more detail later.

It is difficult to compare the results of the polymers with uniform and non-uniform T6T6T at the same $PTMO_{1000}$/DMT length, because there is a large difference in molecular weight. When the inherent viscosity is lower than 2.0 the properties seem to change. The crystallinity seems to increase while the polymers become less elastic. Also the crystallinity of PTMO seems to be enhanced when the molecular weight of a copolymer decreases. As a result the polymers with low molecular weight are less transparent. The influence of molecular weight will be studied in more detail in the near future.

The inherent viscosity of T6T6T–$(PTMO_{1000}/DMT)_{6000}$ (1.9 dl/g) with non-uniform T6T6T (series 3) is high enough to allow comparison of the DMA data with that of series 2. In Fig. 9 the storage moduli of T6T6T–$(PTMO_{1000}/DMT)_{6000}$ with uniform and non-uniform T6T6T are compared.

From Fig. 9 it can be concluded that using non-uniform T6T6T has no effect on the glass transition temperature or rubbery plateau. Therefore, the phase separation and the

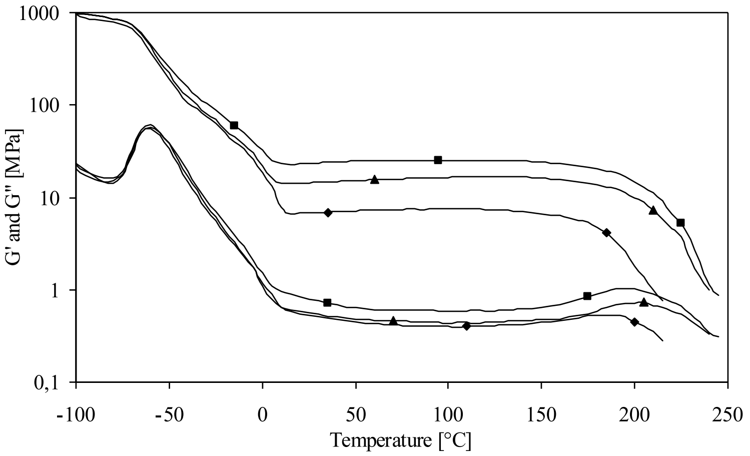

Fig. 8. Storage and loss modulus of T6T6T–(PTMO$_{1000}$/DMT) copolymers with different soft segment lengths and T6T6T with a uniformity of 76% (series 3): (■), T6T6T–(PTMO/$_{1000}$DMT)$_{3000}$; (▲), T6T6T–(PTMO/$_{1000}$DMT)$_{4000}$; (◆), T6T6T–(PTMO/$_{1000}$DMT)$_{6000}$.

crystallinity of T6T6T are the same. The rubbery plateau remains flat because there are only T(6T)$_n$ units with a higher melting temperature ($n > 2$) present and not for example T6T units that melt at a lower temperature. Therefore, the only difference can be seen at the flow temperature. The flow temperature is sharper and therefore, lower with uniform T6T6T as compared to non-uniform T6T6T. This is due to the presence of longer T(6T)$_n$ segments (such as T6T6T6T) in the non-uniform T6T6T. These longer segments will form thicker crystalline lamellae with a higher melting temperature [17]. A disadvantage of this higher and broader flow temperature is that the processing temperature for the polymer with non-uniform T6T6T is higher. As a result there is more chance for thermal degradation.

3.2.4. Glass transition temperature

In Fig. 10 the glass transition temperature of the PTMO(/DMT) phase is given as function of the hard segment content for T6T6T–PTMO(/DMT) (series 1–3) and TΦT–PTMO(/DMT) copolymers.

The glass transition temperature is near the T_g of pure PTMO (−86 °C) [26] for copolymers of PTMO and T6T6T (series 1) or TΦT [14]. With extended PTMO$_{1000}$/DMT and TΦT the T_g is increased to −65 °C and with T6T6T to −63 to −60 °C. Apparently PTMO$_{1000}$/DMT has a little higher T_g than PTMO because the flexibility decreases by incorporation of a terephthalic unit. The explanation is consistent with the observation that the T_g is almost independent of the hard segment content.

The somewhat higher T_g of PTMO$_{1000}$/DMT in the copolymers with T6T6T compared to TΦT might be caused by less complete crystallisation of T6T6T. As a result more T6T6T units are mixed with the amorphous PTMO$_{1000}$/ DMT phase which decreases the mobility. It could also be that more hydrogen bonding between T6T6T and terephthalic units in PTMO$_{1000}$/DMT is possible than with TΦT, which increases the stiffness of this phase as well.

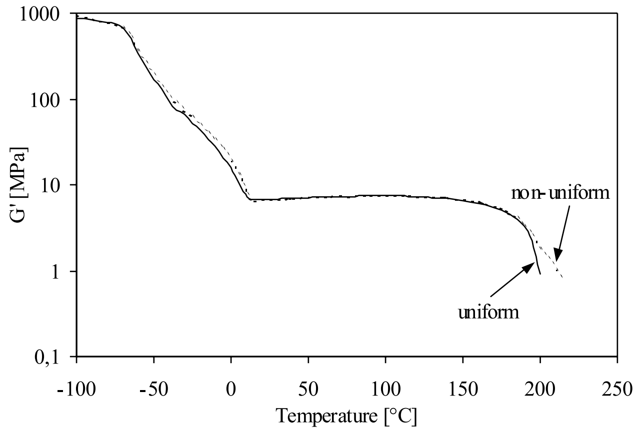

Fig. 9. Storage modulus of T6T6T–(PTMO$_{1000}$/DMT)$_{6000}$: (—), series 2 (uniform T6T6T, 2.0 dl/g); (- - -), series 3 (non-uniform T6T6T, 1.9 dl/g).

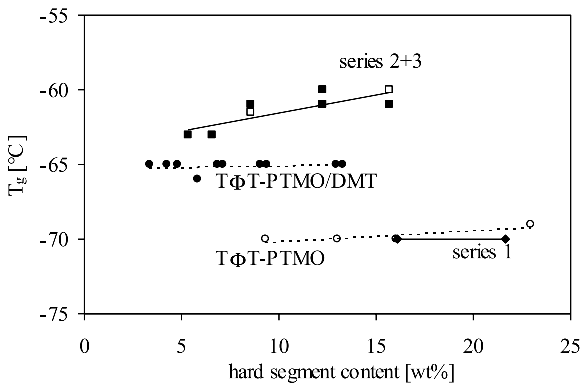

Fig. 10. Glass transition temperature of PTMO(/DMT) as function of hard segment content: (◆), T6T6T–PTMO, series 1; (■), T6T6T–(PTMO$_{1000}$/DMT), series 2; (□), T6T6T–(PTMO$_{1000}$/DMT), series 3, non-uniform; (○), TΦT–PTMO [14]; (●), TΦT–PTMO$_{1000}$/DMT [15].

3.2.5. Rubber modulus

In Fig. 11 the rubber modulus for T6T6T–PTMO(/DMT) with T6T6T (series 1–3) is given as a function of the hard segment content. The modulus of the rubbery plateau at 25 °C with T6T6T is compared with that of polymers with TΦT as a hard segment.

Fig. 11 shows that the logarithm of the modulus at room temperature (G'(25 °C)) increases with the T6T6T and TΦT content. With TΦT a linear increase of rubber modulus with TΦT content was found. According to Wegner [30], the logarithm of the modulus in the rubbery plateau of a segmented copolymer follows a linear relationship with the crystallinity. Eq. (2) describes this relationship where E is the modulus, E_c is the modulus of the crystalline fraction, E_a is the modulus of the amorphous fraction and x_c is the crystallinity.

$$\log E = \log E_a + x_c \log \frac{E_c}{E_a} \qquad (2)$$

The effect of increasing hard segment content on the modulus is strong. The strong increase in modulus with T6T6T and TΦT content is probably due to the formation of threads or ribbons of crystalline units that act as reinforcing fillers for the amorphous matrix [6]. The copolymers with T6T6T as crystallisable units with high inherent viscosity (>2 dl/g) follow the line for TΦT. With T6T6T the copolymers with an inherent viscosity of ~1.5 dl/g have a higher rubber modulus. This suggests that the crystallisation is better and more complete or more effective when the molecular weight is not too high (around 1.4–1.6 dl/g).

A linear relationship between rubber modulus and T6T6T content is drawn for T6T6T using the points with maximum crystallinity and the intercept for TΦT–PTMO(/DMT) copolymers (1.3 MPa). When it is assumed that the crystallinity is 100% in these copolymers the following relation between rubber modulus and crystallinity can be set:

$$G'(25\ °\mathrm{C}) = 1.3 \exp(0.21 x_c) \qquad [\mathrm{MPa}] \qquad (3)$$

With Eq. (3) the crystallinity (x_c; wt% crystalline T6T6T) and crystallinity of T6T6T (crystalline T6T6T content x_c/ T6T6T content) in the copolymers of series 1–3 can be calculated. The results can be found in Table 2.

The crystallinity of T6T6T in the copolymers is between 72 and 100%, provided that the T6T6T in the copolymers that were assumed to have 100% crystallinity has indeed crystallised completely. When the crystallinity of T6T6T in these reference polymers is somewhat lower than 100%, then the calculated, relative crystallinity of the other copolymers decreases correspondingly.

The effect of the inherent viscosity (molecular weight) on the crystallisation of T6T6T is as yet unclear. It seems that the crystallinity of T6T6T is higher when the inherent viscosity is below 2 dl/g.

3.2.6. Flow temperature

In Fig. 12 the flow temperature for T6T6T–PTMO(/DMT) with uniform T6T6T (series 1 and 2) is given as function of the hard segment content. The copolymers with non-uniform T6T6T have a higher flow temperature due to the presence of thicker crystalline lamellae [17]. These results are not incorporated in Fig. 12. The flow temperature with T6T6T is compared with that of copolymers with TΦT as crystallisable segment.

The flow temperature decreases with decreasing hard segment content. This phenomenon has been explained by the solvent effect theory of Flory [14,29] (Eq. (4)). According to this theory a decrease in the melting temperature can mainly be ascribed to differences in the molar fraction of crystalline units. With decreasing T6T6T content the molar fraction decreases and thus the melting

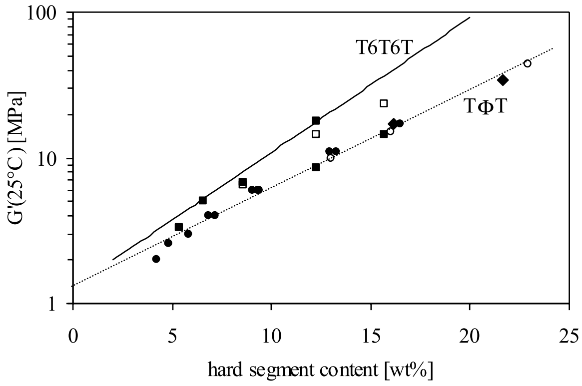

Fig. 11. Modulus at room temperature as function of hard segment content: (◆), T6T6T–PTMO, series 1; (■), T6T6T–(PTMO$_{1000}$/DMT), series 2; (□), T6T6T–(PTMO$_{1000}$/DMT), series 3, non-uniform; (○), TΦT–PTMO [14]; (●), TΦT–PTMO$_{1000}$/DMT [15].

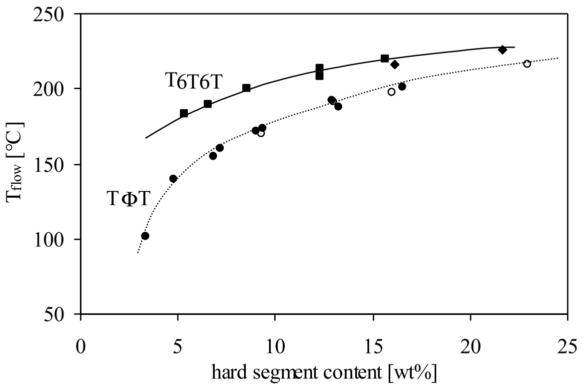

Fig. 12. Flow temperature ($G' = 1$ MPa) as function of hard segment content: (◆), T6T6T–PTMO, series 1; (■), T6T6T–(PTMO$_{1000}$/DMT), series 2; (○), TΦT–PTMO [14]; (●), TΦT–PTMO$_{1000}$/DMT [15].

Table 2
Degree of crystallinity as calculated with Eq. (3) and crystallinity of T6T6T in T6T6T–PTMO(/DMT) copolymers of series 1–3

	η_{inh} (dl/g)	G'(25°C) (MPa)	T6T6T content (wt%)	Crystalline content (wt%)	Crystallinity T6T6T (%)
Series 1: uniform					
T6T6T–$PTMO_{2000}$	2.2	34	21.7	16	72
T6T6T–$PTMO_{2900}$	2.7	17	16.1	12	76
Series 2: uniform					
T6T6T–$(PTMO_{1000}/DMT)_{3000}$	3.1	14.5	15.7	11	73
T6T6T–$(PTMO_{1000}/DMT)_{4000}$	1.4	18	12.3	12	100
T6T6T–$(PTMO_{1000}/DMT)_{4000}$	2.3	8.5	12.3	8	73
T6T6T–$(PTMO_{1000}/DMT)_{6000}$	2.6	6.8	8.6	7	92
T6T6T–$(PTMO_{1000}/DMT)_{8000}$	2.2	5.1	6.6	5	99
T6T6T–$(PTMO_{1000}/DMT)_{10,000}$	2.5	3.3	5.4	3	83
Series 3: non-uniform					
T6T6T–$(PTMO_{1000}/DMT)_{3000}$	1.4	23.5	15.7	14	88
T6T6T–$(PTMO_{1000}/DMT)_{4000}$	1.5	14.3	12.3	11	93
T6T6T–$(PTMO_{1000}/DMT)_{6000}$	1.9	6.9	8.6	7	93

temperature and flow temperature decrease:

$$\frac{1}{T_m} - \frac{1}{T_m^0} = \frac{R}{\Delta H_m^0}\frac{V_p}{V_s}(v_1 - \chi v_1^2) \qquad [\mathrm{MPa}] \qquad (4)$$

with:

T_m, observed melting temperature of the copolymer
T_m^0, theoretical melting temperature of the homopolymer of the crystallisable unit
R, gas constant
ΔH_m^0, theoretical heat of fusion
V_p, molar volume of the crystalline segment
V_s, molar volume of the solvent (amorphous segment)
χ, Flory interaction parameter
v_1, volume fraction of diluent (amorphous segment).

The flow temperature of the copolymer is higher for T6T6T than for TΦT as a crystalline segment at the same hard segment content, although the melting temperature of TΦT-dimethyl (371 °C) [14] is higher than that of T6T6T-dimethyl (303 °C) [26]. The solvent effect of the amorphous PTMO phase is less for T6T6T than for TΦT. This is due to the lower molar volume and higher lamellar thickness of crystalline ribbons of T6T6T. The more the segment length approaches that of the homopolymer of the crystalline segment, the smaller the solvent effect of the amorphous phase. Another effect could be the higher interaction of PTMO and T6T6T compared to PTMO and TΦT.

3.3. DSC

With DSC the melting and crystallisation temperatures of several T6T6T–PTMO(/DMT) copolymers of series 1 and 2 were determined. The melting enthalpy of T6T6T-dimethyl was 152 J/g. The melting enthalpy of T6T6T in the copolymers can be calculated from the T6T6T content and with these values the crystallinity can roughly be calculated. The results are given in Table 3. Fig. 13 shows the second heating and cooling scan of T6T6T–$(PTMO_{1000}/DMT)_{4000}$ (series 2).

The melting temperature as measured by DSC is a little higher than the flow temperature as determined by DMA. At the flow temperature the polymer is not yet completely molten. The melting peak is quite broad and seems to show a shoulder at the high temperature side.

The crystallisation curve shows two peaks, one around 190 °C and one around 135 °C. The second peak can probably be attributed to a crystalline transition. Such a crystalline transition was also found for 6T6-diamine [26], and is quite common for polyamides [31,32]. However, T6T6T-dimethyl did not show such a crystalline transition in DSC [26].

The undercooling ($T_m - T_c$) is only 23–24 °C for the copolymers with extended $PTMO_{1000}$/DMT. This indicates that the crystallisation of T6T6T in these polymers is very fast. It seems that with increasing T6T6T content and with regular PTMO, the rate of crystallisation decreases somewhat.

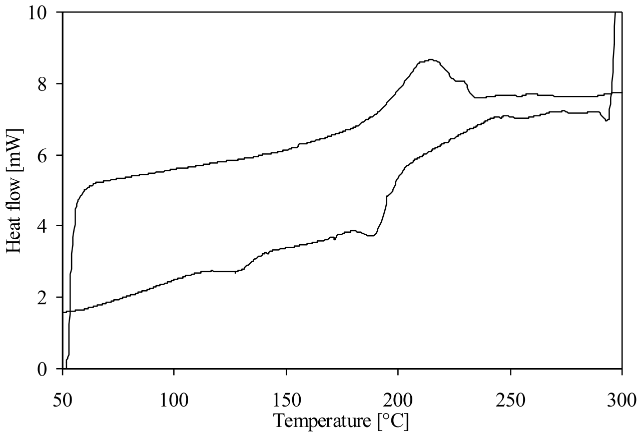

Fig. 13. DSC second heating scan and first cooling scan for T6T6T–$(PTMO_{1000}/DMT)_{4000}$ (series 2) at 20 °C/min.

Table 3
DSC results for several polymers of series 1 and 2 with uniform T6T6T segments at a heating and cooling rate of 20 °C/min

	T6T6T content (wt%)	T_{flow} (°C)	T_m (°C)	ΔH_m (J/g)	ΔH_m (J/g T6T6T)	Cryst.[a] (%)	T_c[b] (°C)	ΔH_c[b] (J/g)	$T_m - T_c$ (°C)
Series 1: uniform									
T6T6T–$PTMO_{2000}$	22	226	227	20	91	60	186; 142	8; 2	40
T6T6T–$PTMO_{2900}$	16	217	220	16	100	66	187; 141	5; 2	33
Series 2: uniform									
T6T6T–$(PTMO_{1000}/DMT)_{3000}$	16	220	222	16	102	67	198; 133	10; 2	24
T6T6T–$(PTMO_{1000}/DMT)_{4000}$	12	208	213	12	98	65	190; 126	6; 1	23

[a] The crystallinity of T6T6T was calculated with the melting enthalpy of T6T6T-dimethyl (152 J/g).

[b] First the peak crystallisation temperature and enthalpy of the main crystallisation peak are given. Second, the corresponding data for the second peak at lower temperature are given.

The crystallinities as calculated from the enthalpy of melting of T6T6T in the copolymer compared to the starting material T6T6T-dimethyl are somewhat lower (about 10%) than the crystallinities that were calculated from the modulus in the rubbery plateau (Table 2). This could be due to the fact that the T6T6T unit has a different enthalpy of melting than T6T6T-dimethyl.

3.4. Compression set

The CS at 20 and 70 °C was measured with polymer pieces, cut from the injection moulded bars. The samples were compressed for 24 h to 25 or 55%. The CS for T6T6T–PTMO(/DMT) polymers with uniform and non-uniform T6T6T segments (series 1–3) are given in Table 4.

The CS at 25% is almost independent of the hard segment content. The CS as function of the rubber modulus for 55% compression at 20 and 70 °C is given in Fig. 14. In these figures the CS data of T6T6T–PTMO (/DMT) of series 1–3 are compared with that of TΦT–PTMO(/DMT).

The CS of T6T6T–PTMO(/DMT) copolymers at 20 °C is very low. Copolymers with T6T6T instead of TΦT show better elastic properties over the whole hard segment content range. Also the copolymers based on T6T6T as a hard segment can be applied over a larger hard segment content range with good elasticity because the CS is less dependent on the hard segment content. A CS of only 6–7% at 20 °C is very favourable for several kinds of applications.

The CS at 20 °C decreases slightly with decreasing rubber modulus and thus with decreasing crystallinity (series 1–3). When the crystallinity is lower, there is less plastic deformation during compression, and therefore, less permanent damage. The data at 20 °C suggest that the CS would decrease even further with lower T6T6T content. For TΦT–PTMO(/DMT) [6] a minimum in the CS at 10–12 wt% hard segment content is observed, and this was explained by the fact that at very low hard segment concentrations the physical crosslink density is too low to prevent plastic flow in this compression test. Such a minimum is not observed for T6T6T–PTMO(/DMT) for concentrations down to 5 wt%.

Table 4
Compression set for T6T6T–PTMO (series 1), T6T6T–($PTMO_{1000}$/DMT) with uniform (series 2) and non-uniform T6T6T (series 3)

	T6T6T content (wt%)	η_{inh} (dl/g)	G'(25 °C) (MPa)	$CS_{25\%}$(20 °C) (%)	$CS_{55\%}$(20 °C) (%)	$CS_{25\%}$(70 °C) (%)	$CS_{55\%}$(70 °C) (%)
Series 1: uniform							
T6T6T–$PTMO_{2000}$	21.7	2.2	34	–	14	–	36
T6T6T–$PTMO_{2900}$	16.1	2.7	17	–	9	–	29
Series 2: uniform							
T6T6T–$(PTMO_{1000}/DMT)_{3000}$	15.7	3.1	14.5	7	10	32	32
T6T6T–$(PTMO_{1000}/DMT)_{4000}$	12.3	2.3	18	7	8	24	34
T6T6T–$(PTMO_{1000}/DMT)_{4000}$	12.3	1.4	8.5	11	18	39	45
T6T6T–$(PTMO_{1000}/DMT)_{6000}$	8.6	2.6	6.8	7	9	21	29
T6T6T–$(PTMO_{1000}/DMT)_{8000}$	6.6	2.2	5.1	6	7	22	34
T6T6T–$(PTMO_{1000}/DMT)_{10,000}$	5.4	2.5	3.3	6	6	24	33
Series 3: non-uniform							
T6T6T–$(PTMO_{1000}/DMT)_{3000}$	15.7	1.4	23.5	10	12	23	24
T6T6T–$(PTMO_{1000}/DMT)_{4000}$	12.3	1.5	14.3	–	8	–	21
T6T6T–$(PTMO_{1000}/DMT)_{6000}$	8.6	1.9	6.9	6	7	18	20

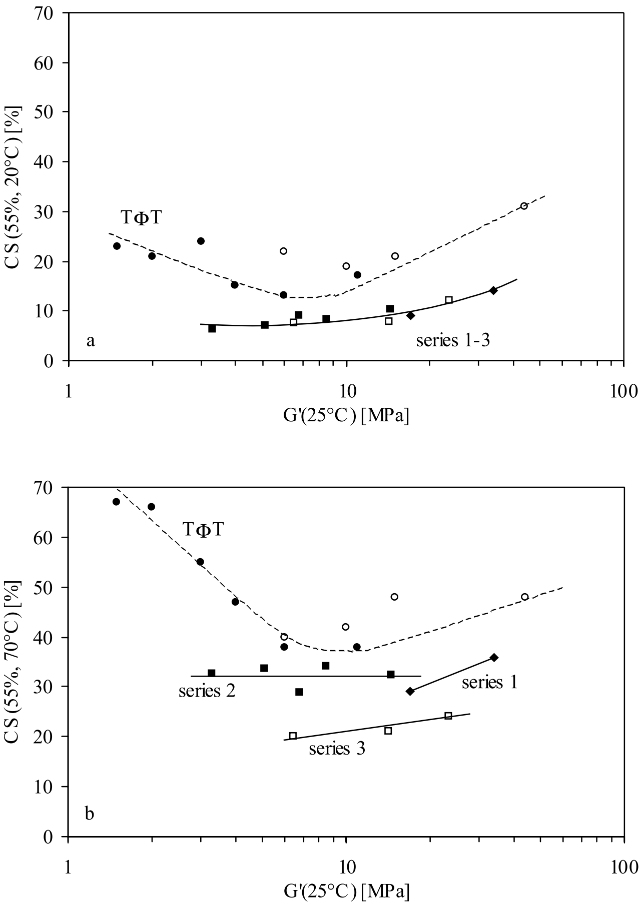

Fig. 14. Compression set (55% compression) at (a) 20 °C and (b) 70 °C as function of the rubber modulus: (◆), T6T6T–PTMO, series 1; (■), T6T6T–(PTMO$_{1000}$/DMT), series 2; (□), T6T6T–(PTMO$_{1000}$/DMT), series 3, non-uniform; (○), TΦT–PTMO [6]; (●), TΦT–PTMO$_{1000}$/DMT [6].

The CS at 70 °C is higher than at 20 °C for copolymers with T6T6T or TΦT as crystallisable segment, but still low. For these copolymers the melting temperature is at 70 °C not reached by far, and thus plastic flow is still suppressed. At 70 °C there is some difference between the three series based on T6T6T. For series 1 and 2 the CS seems almost independent of hard segment content, although there is some spread in the data points. It is remarkable that the polymers of series 3 with non-uniform T6T6T show a lower CS at 70 °C than the polymers with uniform T6T6T. At room temperature there is no difference. This is possibly caused by the lower molecular weight of the copolymers of series 3, but more research is necessary to investigate this. It could also be a result of the presence of thicker crystallites based on longer T6T6T6T or T6T6T6T6T.

The better elasticity in copolymers with T6T6T instead of TΦT over the whole hard segment content range can have several causes. It can be a result of the larger thickness of the T6T6T lamellae as compared to the TΦT lamellae. As a result it will be more difficult to shear the T6T6T lamellae. It could also be a result of the larger PTMO length at a certain hard segment content for T6T6T. The deformation should then mainly take place in the PTMO phase.

The CS (55% compression) at 20 °C is given as a function of 1000/PTMO (in which PTMO is the PTMO(/DMT) length) in Fig. 15. The figure shows that the CS of T6T6T–PTMO(/DMT) copolymers decreases with decreasing 1000/PTMO or with increasing PTMO(/DMT) length. The decrease becomes less steep below PTMO(/DMT) values of 0.4 (PTMO(/DMT) length above 2500 g/mol).

Above a 1000/PTMO value of 0.4 the CS values of T6T6T–PTMO(/DMT) copolymers seem to be comparable with that of TΦT–PTMO(/DMT) copolymers. These data follow a line that crosses the origin. This suggests that the length of the amorphous segment and not the hard segment type and content determines the CS below a PTMO(/DMT) length of $\sim$3000 g/mol. Apparently the deformation takes place mainly in the PTMO phase.

Below a 1000/PTMO value of 0.4 (PTMO(/DMT) length above 2500 g/mol) the CS values of T6T6T–PTMO(/DMT) copolymers are lower than that of TΦT–PTMO(/DMT) copolymers. For TΦT systems [6] at low TΦT content the CS was thought to increase because the crystalline content is too low to prevent plastic flow. Apparently the thicker T6T6T ribbons are more effective or less deformed in compression than the thin TΦT crystalline ribbons. This figure also suggests that even lower CS values could be obtained, probably by increasing the lamellar thickness of the crystalline ribbons. At higher lamellar thickness the PTMO length between two crystalline ribbons at constant hard segment content is higher.

The low uniformity of T6T6T in series 3 does not seem to have a negative effect on the properties. With a uniformity of 76% the crystallinity is still high (Table 2) and the properties of T6T6T–(PTMO$_{1000}$/DMT) copolymers are

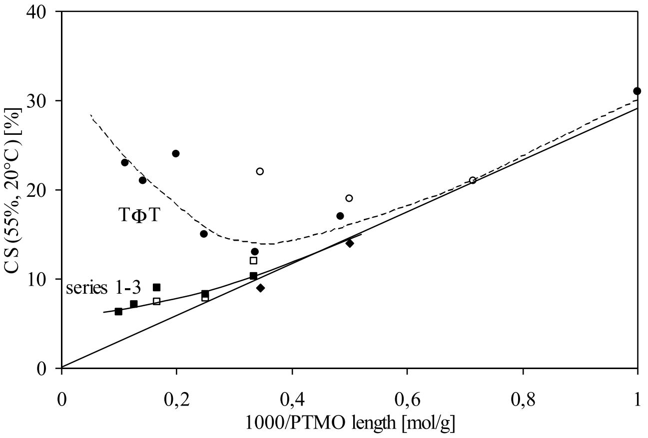

Fig. 15. Compression set (55% compression) at 20 °C as function of 1000/PTMO (the PTMO(/DMT) length): (◆), T6T6T–PTMO, series 1; (■), T6T6T–(PTMO$_{1000}$/DMT), series 2; (□), T6T6T–(PTMO$_{1000}$/DMT), series 3, non-uniform; (○), TΦT–PTMO [6]; (●), TΦT–PTMO$_{1000}$/DMT [6].

comparable with that using uniform T6T6T. It was expected that the properties would be better in the copolymers based on uniform T6T6T [7–10]. Apparently the uniformity of T6T6T is not important as long as it is above a certain value (at least 76%).

3.5. AFM

The morphology of several T6T6T–(PTMO$_{1000}$/DMT) copolymers based on uniform T6T6T (series 2) was studied by AFM. In Fig. 16 the morphology of T6T6T–(PTMO$_{1000}$/DMT)$_{6000}$ (sample cooled down from the melt) and in Fig. 17 of T6T6T–(PTMO$_{1000}$/DMT)$_{3000}$ (solution cast sample from NMP) is given. Each figure shows a height and phase image. The phase image corresponds to a picture of the hardness of the sample over the measured area. The crystallinity in the picture seems higher because of measurement is not only on the surface.

The AFM pictures (phase images) show a well-defined morphology of hard threads or ribbon-like structures of T6T6T in a soft amorphous matrix. The threads are not very long for the melt sample of T6T6T–(PTMO$_{1000}$/DMT)$_{6000}$. The solution cast sample of T6T6T–(PTMO$_{1000}$/DMT)$_{3000}$ shows threads that are very long (up to 0.5 μm) and also some spherulitic structures. This is probably due to the high T6T6T content in these copolymers.

In the height images the individual threads are visible as well, especially at the 1 × 1 μm^2 picture. It seems that the samples contain clusters of T6T6T threads, so the threads are not randomly distributed. The clusters are larger for the solution cast sample of T6T6T–(PTMO$_{1000}$/DMT)$_{3000}$ than for the melt sample of T6T6T–(PTMO$_{1000}$/DMT)$_{6000}$. Both the higher concentration of T6T6T and the method of sample preparation are probably responsible for this.

3.6. WAXD

With wide angle X-ray diffraction (WAXD) the morphology of the crystalline phase of a melt-pressed strip of 1 mm thickness of T6T6T–(PTMO$_{1000}$/DMT)$_{3000}$ was measured. The WAXD diagram of the copolymer is compared with that of T6T6T-dimethyl [26] in Fig. 18.

The amorphous PTMO phase in T6T6T–(PTMO$_{1000}$/DMT)$_{3000}$ gives a broad peak in the area where the main crystallisation peak of T6T6T is expected (around 23°). Other small peaks in T6T6T–(PTMO$_{1000}$/DMT)$_{3000}$ at $2\Theta = 8$, 26, 29 and 42° correspond nicely with peaks of T6T6T-dimethyl.

3.7. Comparison with other systems

The T6T6T and TΦT based segmented copolymers are copolyether–esteramides, a special type of the thermoplastic copolyether–amides (TPE-A). These materials are new compared to the commercial materials that are described here, as they consist of uniform hard, crystallisable segments.

The commercial material Arnitel® is a segmented copolyether–ester (TPE-E) based on a PBT–PTMO copolymer. Desmopan® is a commercial thermoplastic polyurethane (TPE-U), based on polyether soft segments.

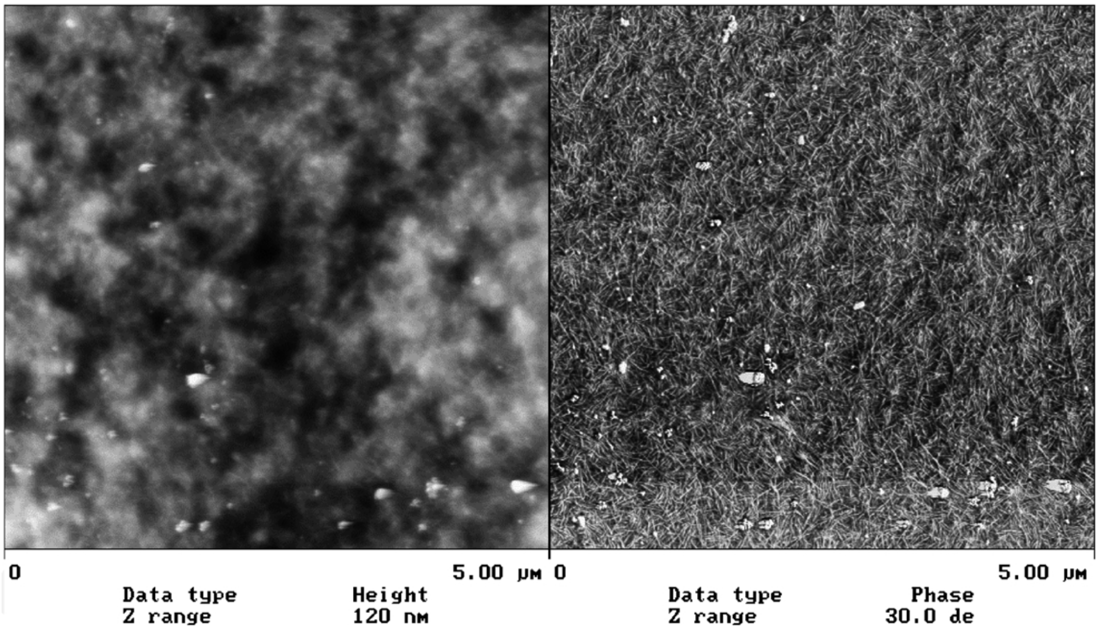

Fig. 16. Morphology as measured by AFM at 5 × 5 μm^2 for a melt sample of T6T6T–(PTMO$_{1000}$/DMT)$_{6000}$ (series 2, 9 wt% T6T6T) taken from the reactor side; (left, height image; right, phase angle image).

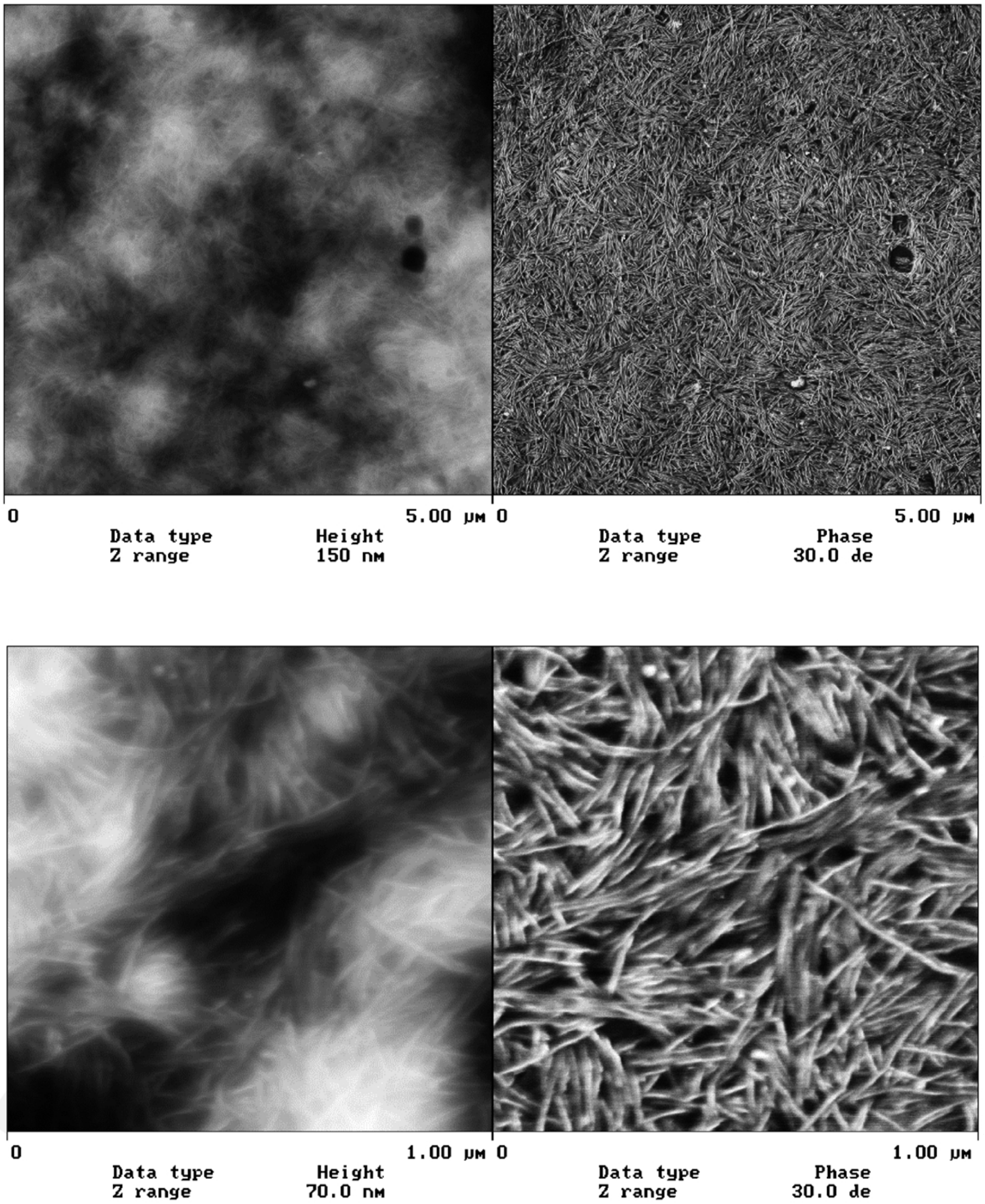

Fig. 17. Morphology as measured by AFM at 5×5 μm^2 and 1×1 μm^2 for a solution cast sample of T6T6T–(PTMO$_{1000}$/DMT)$_{3000}$ (series 2, 16 wt% T6T6T); (left, height image; right, phase angle image).

In both materials the hard segments are not of uniform length. The properties of a hard and a soft grade of these commercial materials were evaluated [33].

The T6T6T–PTMO(/DMT) copolymers that are described in this article are compared with the TΦT–PTMO(/DMT) copolymers from previous research [6, 14–16] and several commercial thermoplastic elastomers [33] in Table 5.

With T6T6T and extended PTMO$_{1000}$/DMT, a TPE with very good properties such as sharp transition temperatures and a very wide and constant rubbery plateau can be obtained, comparable to the copolymers with TΦT as crystallisable segment, but with a higher melting temperature and lower CS. Another advantage of copolymerisation with T6T6T instead of TΦT is that the products are less coloured, due to the absence of aromatic amines. Therefore, the use of T6T6T is preferred over the use of TΦT in segmented copolymers. The materials also have good melt processability and can be recycled. Therefore, the new T6T6T–(PTMO$_{1000}$/DMT) materials are very interesting

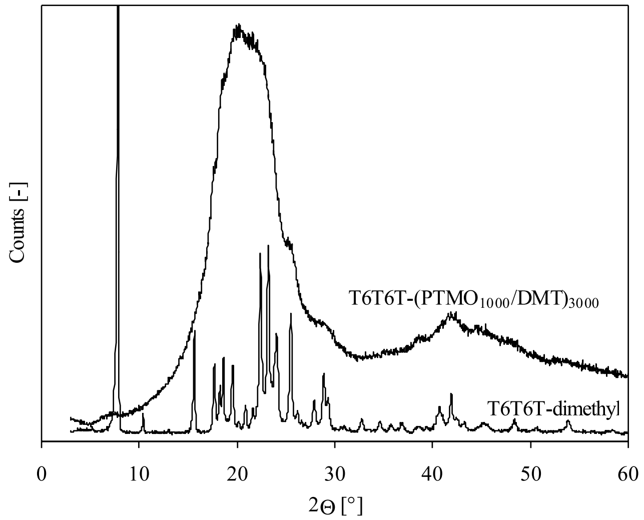

Fig. 18. WAXD data of T6T6T–$(PTMO_{1000}/DMT)_{3000}$ (series 2) compared to T6T6T-dimethyl [26].

for TPE applications similar to Arnitel® and Desmopan®. T6T6T–$(PTMO_{1000}/DMT)$ is a TPE with a constant modulus over a wider temperature range and lower CS. The properties of this polymer can be easily tuned as desired by changing the PTMO(/DMT) length.

It is expected that the properties of T6T6T–PTMO(/DMT) copolymers can probably be changed and optimised in several ways: the choice of the soft segment type and length, the polymerisation reaction conditions, the processing conditions and by using additives. The synthesis would become more economically feasible when it can be performed in the melt, so when the T6T6T segment is formed in situ, for example by starting from 6T6-diamine or even by starting from 1,6-hexamethylenediamine. This is however, at the cost of uniformity of the T6T6T in the copolymer, but it was shown that a uniformity of 76% is sufficient for good properties. Another interesting modification would be to use other tetra-amides as crystallisable segment instead of T6T6T, for example T4T4T [26]. The melting temperature of nylon-4,T is 60 °C higher than that of nylon-6,T [28] and therefore, the melting temperature of a copolymer with T4T4T instead of T6T6T is expected to be maximal 60 °C higher. So, with this segment it is possible to increase the melting temperature of the polymer and to make the rubbery plateau even wider while keeping a low modulus and good elasticity. Also optimisation of the processing of the polymer, for example by injection moulding, can lead to better properties.

4. Conclusions

Segmented copolymers based on T6T6T-dimethyl and $PTMO_{1000}/DMT$ that are thermoplastic elastomers can be made via a polycondensation reaction. Copolymers with different soft segment types and lengths and with uniform and non-uniform T6T6T were studied. With DMA experiments it was shown that the polymers all have a low glass transition temperature (−60 to −70 °C). The glass transition temperature of PTMO is lower for regular PTMO than for DMT extended $PTMO_{1000}$. With regular PTMO of >2000 g/mol crystallisation of PTMO occurs. The rubbery plateau of all copolymers is wide and extremely flat and the melting temperature is sharp and high when uniform T6T6T is used. With non-uniform T6T6T the flow temperature is somewhat broadened. The modulus of the rubbery plateau and the flow temperature increase with increasing T6T6T content and thus with increasing crystallinity. The modulus of T6T6T–$(PTMO_{1000}/DMT)$ increases from 3.3–14.5 MPa and the flow temperature from 183–220 °C when the $PTMO_{1000}/DMT$ length is decreased from 10,000–3000 g/mol (5–16 wt% T6T6T). The modulus is not dependent on the PTMO length or network density but on the crystallinity. The content of reinforcing crystalline ribbons in the amorphous matrix determines the modulus. The crystallinity of T6T6T

Table 5
Comparison of T6T6T–PTMO(/DMT) segmented copolymers with other systems

	Hard segment (wt%)	G'(25 °C) (MPa)	T_{flow} (°C)	T_g (°C)	$CS_{55\%}$(20 °C) (%)	$CS_{55\%}$(70 °C) (%)
T6T6T–PTMO(/DMT) (series 1 and 2)						
T6T6T–$PTMO_{2000}$	22	34	226	−70	14	36
T6T6T–$(PTMO_{1000}/DMT)_{3000}$	16	14.5	225	−61	10	32
T6T6T–$(PTMO_{1000}/DMT)_{4000}$	12	8.5	208	−60	8	34
TΦT–PTMO(/DMT) [6,14–16]						
TΦT–$PTMO_{2000}$	13	10	191	−65	19	42
TΦT–$(PTMO_{1000}/DMT)_{3000}$	9	6	172	−65	15	47
TΦT–$(PTMO_{1000}/DMT)_{4000}$	7	4	155	−65	24	55
Commercial polymers [33]						
Arnitel® EM400	–	18	182	−70	15	36
Arnitel® EL550	–	67	205	−50	30	58
Desmopan® KU-8672	–	11	150	−45	13	41
Desmopan® 955u	-	91	176	−31	23	60

in injection moulded test bars as calculated from their rubber modulus is between 70 and 100%.

The undercooling, as measured by DSC, is 20–30 °C, which is low compared to other semi-crystalline polymers. The crystallinity of T6T6T as calculated from the melting enthalpy of the polymers is about 10% lower than that calculated from the rubber modulus. The CS at room temperature is low (6–7%) and decreases slightly with decreasing T6T6T content. The uniformity of T6T6T, when it is at least 76%, does not have much influence on the polymer properties, except for the flow temperature. With AFM it was confirmed that the crystalline T6T6T units form long threads or ribbon like structures with a high aspect ratio in the amorphous PTMO matrix.

This type of thermoplastic elastomers is very interesting for application as TPE. The segmented copolymers show a good combination of properties as they have a good elasticity, are melt-processable (and can be recycled), have a high modulus, have a good solvent resistance, are transparent and are dimensional stable up to high temperatures.

Acknowledgements

C. Padberg (University of Twente) is acknowledged for performing the AFM measurements and H. Koster (University of Twente) is acknowledged for performing the WAXD measurements.

References

[1] Holden G, Legge NR, Quirk R, Schroeder HE, editors. Thermoplastic elastomers, 2nd ed. Hanser: Hanser Publishers; 1996.

[2] Grady BP, Cooper SL. In: Mark JE, Erman B, Eirich FR, editors. Science and technology of rubber. San Diego: Academic Press; 1978. Chapter 13.

[3] Zhu L, Wegner G. Makromol Chem 1981;182:3625.

[4] Sauer BB, McLean RS, Thomas RR. Polym Int 2000;49:449.

[5] Cella RJ. J Polym Sci: Symp 1973;42:727.

[6] Niesten MCEJ, Gaymans RJ. Polymer 2001;42:6199.

[7] Harrell LL. Macromolecules 1969;2:607.

[8] Ng HN, Allegrazza AE, Seymour RW, Cooper SL. Polymer 1973;14: 255.

[9] Eisenbach CD, Baumgartner M, Gunter G. In: Lal J, Mark JE, editors. Advances in elastomer and rubber elasticity, proceedings symposium, vol. 51. New York: Plenum Press; 1985.

[10] Miller JA, Shaow BL, Hwang KKS, Wu KS, Gibson PE, Cooper SL. Macromolecules 1985;18(1):32.

[11] Sorta E, Della Fortuna G. Polymer 1980;21:728.

[12] Gaymans RJ, De Haan JL. Polymer 1993;34:4360.

[13] Bouma K, Wester GA, Gaymans RJ. J Appl Polym Sci 2001;80:1173.

[14] Niesten MCEJ, Feijen J, Gaymans RJ. Polymer 2000;41:8487.

[15] Niesten MCEJ, Ten Brinke JW, Gaymans RJ. Polymer 2001;42:1461.

[16] Niesten MCEJ, Krijgsman J, Gaymans RJ. J Appl Polym Sci 2001;82: 2194.

[17] Hoffman JD, Weeks JJ. J Res Nail Bur Stand, Sect A 1962;66:13.

[18] Niesten MCEJ, Harkema S, Van der Heide E, Gaymans RJ. Polymer 2001;42:1131.

[19] Garcia D, Starkweather H. J Polym Sci Phys Ed 1985;32:537.

[20] Ramesh C, Keller A, Eltink SJEA. Polymer 1994;35:5293.

[21] Van Bennekom ACM, Gaymans RJ. Polymer 1997;38:657.

[22] Van Hutten PF, Mangnus RM, Gaymans RJ. Polymer 1993;35:4193.

[23] Niesten MCEJ, Bosch H, Gaymans RJ. J Appl Polym Sci 2001;81: 1605.

[24] Perego G, Cesart M, Della Fortuna G. J Appl Polym Sci 1984;29: 1141.

[25] Guang L, Gaymans RJ. Polymer 1997;3:4891.

[26] Krijgsman J, Husken D, Gaymans RJ. Polymer 2003;44(23):7043.

[27] Dreyfuss P. In: Mark HF, Bikales NM, Overberger CG, Menges G, editors. Encyclopedia of polymer science and engineering. New York: Wiley; 1989. p. 654.

[28] Morgan PW, Kwolek SL. Macromolecules 1975;8:104.

[29] Flory PJ. Trans Faraday Soc 1955;51:848.

[30] Wegner G. In: Legge NR, Holden G, Schroeder HE, editors. Thermoplastic elastomers, 1st ed. Munich: Carl Hanser Verlag; 1987. Chapter 12.

[31] Todoki M, Kawaguchi T. J Polym Sci Phys Ed 1977;15:1067.

[32] Hirschinger J, Miura H, Gardner KH, English AD. Macromolecules 1990;23:2153.

[33] Niesten MCEJ, Gaymans RJ. J Appl Polym Sci 2001;81:1372.